Tkatchenko-Scheffler van der Waals correction method with and without self-consistent screening applied to solids

Tomáš Bučko,[1,2,*] S. Lebègue,[3,†] Jürgen Hafner,[4] and J. G. Ángyán[3]

[1]*Department of Physical and Theoretical Chemistry, Faculty of Natural Sciences, Comenius University, Mlynská Dolina, SK-84215 Bratislava, Slovakia*

[2]*Institute of Inorganic Chemistry, Slovak Academy of Sciences, Dubravska cesta 9, SK-84236 Bratislava, Slovakia*

[3]*Laboratoire de Cristallographie, Résonance Magnétique et Modélisations (CRM2, UMR CNRS 7036) Institut Jean Barriol, Université de Lorraine BP 70239, Boulevard des Aiguillettes 54506 Vandoeuvre-lès-Nancy, France*

[4]*Fakultät für Physik and Center for Computational Materials Science, Universität Wien, Sensengasse, Wien 1090 Austria*

(Received 21 December 2012; published 26 February 2013)

The method proposed by Tkatchenko and Scheffler [Phys. Rev. Lett. **102**, 073005 (2009)] to correct density functional calculations for the missing van der Waals interactions is implemented in the Vienna *ab initio* simulation package (VASP) code and tested on a wide range of solids, including noble-gas crystals, molecular crystals (α-N_2, sulfur dioxide, benzene, naphthalene, cytosine), layered solids (graphite, hexagonal boron nitride, vanadium pentoxide, MoS_2, $NbSe_2$), chain-like structures (selenium, tellurium, cellulose I), ionic crystals (NaCl, KI), and metals (nickel, zinc, cadmium). In addition to the original formulation expressing the van der Waals (vdW) corrections as pairwise potentials whose strength is derived from the rescaled polarizabilities of the neutral free atoms, the self-consistently screened (TS + SCS) [Phys. Rev. Lett. **108**, 236402 (2012)] variant of the method involving electrodynamic response effects has been examined. Analytical expressions for the forces acting on the atoms and for the components of the stress tensor needed for the relaxation of the volume and shape of the unit cell using the TS + SCS method are derived. While the calculated structures are reasonably close to experiment, the van der Waals corrections to the binding energies are often found to be overestimated in comparison with experimental data. The TS + SCS approach leads to significantly better results in some problematic cases, such as the binding energy of graphite. However, there is room for further improvements, in particular for strongly ionic systems.

DOI: 10.1103/PhysRevB.87.064110 PACS number(s): 71.15.−m

I. INTRODUCTION

With its unique combination of low computational cost and reasonable accuracy, density functional theory (DFT) has become the most popular method for calculating total energies, atomic, and electronic structures of molecules and solids in quantum chemistry and condensed matter physics. However, common local and semilocal approximations of the exchange-correlation (xc) energy functional notoriously fail to describe weak intermolecular or van der Waals (vdW) forces. In particular, it is easy to see that such functionals are basically unadapted to grasp long-range correlations between fluctuating electron densities which are responsible for London dispersion forces. Although these forces are much weaker than covalent or ionic interactions, they are crucial for the cohesion of layered materials, of biological macromolecules, molecular crystals, and in many other examples of soft matter. Higher-order methods, such as the random phase approximation (RPA),[1–3] quantum Monte Carlo (QMC) calculations,[4] or many-body perturbation theory (MBPT)[5] have been successful in describing these weak interactions quite accurately. However, the high computational effort necessary for the application of these techniques makes them inappropriate for large-scale calculations, in particular for solids where periodic boundary conditions have to be applied. There have been some promising attempts to develop strongly nonlocal "van der Waals functionals" by Langreth, Lundqvist, and coworkers,[6–8] by Dobson *et al.*,[9–11] and more recently by Vydrov and van Voorhis,[12,13] but so far none of these methods have reached chemical accuracy.[14]

As a reasonable compromise between precision, simplicity, and computational cost, *a posteriori* empirical, semi-empirical or even nonempirical correction schemes have been suggested and applied to correct the DFT energy for the missing dispersion effects. Some of the popular methods are based on parameterized interatomic pair potentials of a damped C_6/R^6 form, with C_6 parameters, van der Waals radii, and damping function fit to the results of high-level quantum-chemical calculations for a set of test molecules.[15–17] More sophisticated approaches were proposed by Becke and Johnson[18,19] and by Sato.[20,21] Recently, Tkatchenko and Scheffler[22] (TS) suggested a method based on the idea that accurate interatomic C_6 (dipole-dipole) dispersion coefficients can be calculated using a London-type formula from rescaled atomic dispersion coefficients and polarizabilities.

The scaling factor is determined by the effective volume occupied by the atom in a molecular or solid environment, obtained by the Hirshfeld partitioning of the electron density in the molecule or in the solid.[23] These pairwise interatomic potentials between "atoms in molecules"(see Sec. II) are used to correct standard DFT energies computed, for instance, at the level of the generalized gradient approximation (GGA) and to perform refined optimizations of the molecular or crystalline geometries. The TS method has attracted considerable interest from the scientific community and has been applied to various physical and biophysical problems.[24–27] A first systematic test, performed on some of the emblematic solid state systems having structural and energetic features that are strongly influenced by London dispersion forces, has been reported by Al-Saidi *et al.*[28] Other applications of the method to extended

systems include, e.g., the adsorption of organic molecules at surfaces,[29] the structural relaxation of kaolinites,[30] and the adsorption of saturated hydrocarbons in acidic zeolites.[31]

Very recently, Tkatchenko *et al.*[32] introduced improved versions of the TS method in which electrodynamic response effects are included via solving the self-consistent screening equation of electrodynamics (TS + SCS) and many-body effects (TS + MBD) are taken into account. To date we are aware of only a few reports on applications of the TS + SCS and TS + MBD methods.[32,33] In this publication we report on our implementation of the TS and TS + SCS methods in the Vienna *ab initio* simulation package (VASP) code[34–38] and test the performance of TS and TS + SCS methods for a wide range of solids. Formulas for dispersion corrections to total-energy gradients and the components of the stress tensor have been derived, in particular for the self-consistent screening (TS + SCS) calculations. They are provided in the Supplemental Material.[47]

II. COMPUTATIONAL DETAILS

In analogy to the PBE-D2 method of Grimme,[16] the dispersion energy corrections of the TS method are computed using pairwise potentials defined as

$$E_{\text{disp}} = -\frac{1}{2}\sum_{A=1}^{N}\sum_{B=1}^{N}\sum_{\boldsymbol{L}}{}' \frac{C_{6AB}}{(r^{AB,L})^6} f_{\text{damp}}(r^{AB,L}), \qquad (1)$$

where $r^{AB,L} = |\boldsymbol{r}^{A,0} - \boldsymbol{r}^{B,L}|$, the summations are over all atoms N and all translations of the unit cell $\boldsymbol{L} = (l_1,l_2,l_3)$, and the prime indicates that $A \neq B$ for $\boldsymbol{L} = 0$. The novel feature of the TS method is the application of the atoms-in-molecules concept to the calculations of the static polarizabilities α_A^{TS} and the dispersion coefficients C_{6AA}^{TS}. In particular, α_A^{TS} and C_{6AA}^{TS} are computed by rescaling of the corresponding quantities calculated for free atoms based on the proportionality between atomic volumes and polarizabilities, i.e.,

$$\alpha_A^{\text{TS}} = \frac{V_A^{\text{eff}}}{V_A^{\text{free}}}\alpha_A^{\text{free}}, \qquad (2)$$

where $\frac{V_A^{\text{eff}}}{V_A^{\text{free}}}$ is the ratio between the effective volume occupied by the atom in a molecular or solid environment (V^{eff}) and the volume of free noninteracting atom (V^{free}). An analogous proportionality holds between the effective dispersion coefficients of the free atoms and the atoms in molecules:

$$C_{6AA}^{\text{TS}} = \left(\frac{V_A^{\text{eff}}}{V_A^{\text{free}}}\right)^2 C_{6AA}^{\text{free}}, \qquad (3)$$

which can be rationalized on the basis of the well-known London dispersion formula.

The atomic volumes are estimated using the Hirshfeld partitioning of the all-electron density:

$$\frac{V_A^{\text{eff}}}{V_A^{\text{free}}} = \frac{\int r^3 w_A(\mathbf{r}) n(\mathbf{r}) d^3\mathbf{r}}{\int r^3 n_A^{\text{free}}(\mathbf{r}) d^3\mathbf{r}}, \qquad (4)$$

where $n_A^{\text{free}}(\mathbf{r})$ is the spherically averaged electron density of the neutral free atomic species A. The Hirshfeld weight $w_A(\mathbf{r})$ is defined with respect to these free atomic densities

$$w_A(\mathbf{r}) = \frac{n_A^{\text{free}}(\mathbf{r})}{\sum_B n_B^{\text{free}}(\mathbf{r})}; \qquad (5)$$

the summation is over all atoms present in the system. We remark that the effective volume formula, including an r^3 radial weighting, suggested originally by Johnson and Becke to rescale polarizabilities,[39] was recently rationalized[40] within the framework of the statistical theory of atoms. The combination rule to define the strength of the dipole-dipole dispersion interaction between unlike species is

$$C_{6AB} = \frac{2C_{6A}C_{6B}}{\left[\frac{\alpha_B}{\alpha_A}C_{6A} + \frac{\alpha_A}{\alpha_B}C_{6B}\right]}. \qquad (6)$$

As in the D2 method of Grimme,[16] a Fermi-type damping function is used to eliminate spurious interactions at too short distances (note that dispersion interactions are defined only between nonoverlapping electron densities):

$$f_{\text{damp}}(r^{AB,L}) = \frac{1}{1 + \exp\left[-d\left(\frac{r^{AB,L}}{s_R R_{AB}^{\text{eff}}} - 1\right)\right]}. \qquad (7)$$

The parameter d is fixed at 20, while the scaling coefficient s_R is specific for the choice of the exchange-correlation functional used in the DFT calculations. In this study we use the value of $s_R = 0.94$ that has been found to be optimal[41] for calculations based on the PBE functional.[42] The parameter R_{AB}^{eff} corresponds to the sum of the atom-in-molecule vdW radii:

$$R_{AB}^{\text{eff}} = R_A^{\text{eff}} + R_B^{\text{eff}}, \qquad (8)$$

which are computed by rescaling the free-atom vdW radii R^{free}:

$$R_A^{\text{eff}} = \left(\frac{\alpha_A^{\text{TS}}}{\alpha_A^{\text{free}}}\right)^{\frac{1}{3}} R_A^{\text{free}}. \qquad (9)$$

While the values of R^{free} are quite well defined for the rare-gas atoms as one half of the separation between the atoms in a relaxed dimer (the atoms in the rare-gas dimers interact exclusively via dispersion and repulsive interactions), for other elements the choice of this parameter is a bit more problematic. The solution proposed by Tkatchenko and Scheffler[22] for any other element consists in taking the value of R_A^{free} as the radius for which the electron density of the free atom is equal to the density at half of the equilibrium distance in a dimer of the noble-gas atom from the same row of the periodic table as the element under consideration. For our calculations, the free-atom parameters kindly provided by the authors of Ref. 22 have been used.[43]

Recently, Tkatchenko *et al.*[32] proposed a computationally efficient way to account for electrodynamic response effects, in particular the interaction of atoms with the dynamic electric field due to the surrounding polarizable atoms. In this method, termed TS + SCS, the frequency-dependent screened polarizability $[\alpha_A^{\text{SCS}}(i\omega)]$ is obtained by solving the self-consistent screening equation:

$$\alpha_A^{\text{SCS}}(i\omega) = \alpha_A^{\text{TS}}(i\omega) - \alpha_A^{\text{TS}}(i\omega)\sum_{A\neq B}\tau_{A,B}\alpha_B^{\text{SCS}}(i\omega), \qquad (10)$$

where $\tau_{A,B}$ is the dipole interaction tensor [see Eq. (6) in the Supplemental Material] and $\alpha_A^{\rm TS}(i\omega)$ is the effective frequency-dependent polarizability, approximated by

$$\alpha_A^{\rm TS}(i\omega) = \frac{\alpha_A^{\rm TS}}{1+(\omega/\omega_A)^2}. \tag{11}$$

The characteristic mean excitation frequency ω_A is computed by the relationship

$$\omega_A = \frac{4}{3}\frac{C_{6AA}^{\rm TS}}{\left(\alpha_A^{\rm TS}\right)^2} \tag{12}$$

from the static polarizability $\alpha_A^{\rm TS}$ and the dispersion interaction coefficient $C_{6AA}^{\rm TS}$ defined in Eqs. (2) and (3), respectively. The dispersion energy is computed from the same equation as in the original TS method [Eq. (1)] but with parameters C_{6AA}, α_A, and R_A calculated using the frequency-dependent polarizability $\alpha_A^{\rm SCS}(i\omega)$. The dispersion coefficients are computed from the Casimir-Polder integral:[44]

$$C_{6AA} = \frac{3}{\pi}\int_0^\infty \alpha_A^{\rm SCS}(i\omega)\alpha_A^{\rm SCS}(i\omega)d\omega, \tag{13}$$

and the van der Waals radii are obtained by rescaling the TS radii as

$$R_A^{\rm SCS} = \left(\frac{\alpha_A^{\rm SCS}}{\alpha_A^{\rm TS}}\right)^{1/3} R_A^{\rm TS}. \tag{14}$$

As in the TS method, the value of the scaling parameter s_R [see Eq. (7)] has been optimized using the S22 training set of molecules.[45] In this work, the scaling parameter $s_R = 0.97$ optimized for the PBE functional[43] has been used.

For the optimizations of the unit cell volume and shape as well as of the atomic positions, we have computed the contributions of the dispersion interactions to the energy gradients and to the stress tensor. Because the C_6 parameter and the damping function depend on the volume ratio $\frac{V_A^{\rm eff}}{V_A^{\rm free}}$, and hence implicitly on the charge density $n(\mathbf{r})$ of the interacting system, the exact expression for energy gradient should involve the indirect derivative of the dispersion contribution, $\frac{\partial E_{\rm disp}}{\partial n(\mathbf{r})}\frac{\partial n(\mathbf{r})}{\partial x}$. In our numerical tests we found that the quantity $\frac{V_A^{\rm eff}}{V_A^{\rm free}}$ and therefore also $E_{\rm disp}$ changes only very slowly under a variation of the charge density. Hence the contribution of this term to energy gradients and stress tensor elements can be neglected. In the TS + SCS method, the explicit dependence of the polarizability matrix on the atomic coordinates gives rise to rather complex expressions for gradients and stress tensor. In our preliminary tests we found that this contribution is significant and cannot be neglected in structural optimizations. The importance of this correction can be illustrated by a simple numerical example. Let us consider a halide crystal (e.g., NaCl) with a simple cubic lattice. Due to symmetry, the cell volume is the only parameter to be optimized. The internal pressure $p^{\rm int}$ (defined as one third of the trace of the stress tensor) can be considered as a generalized force that should vanish in equilibrium. In Fig. 1, the energy versus volume and internal pressure versus volume curves are displayed for calculations performed with and without correction. The volume corresponding to the energy minimum is $V_0 = 168\ \text{Å}^3$.

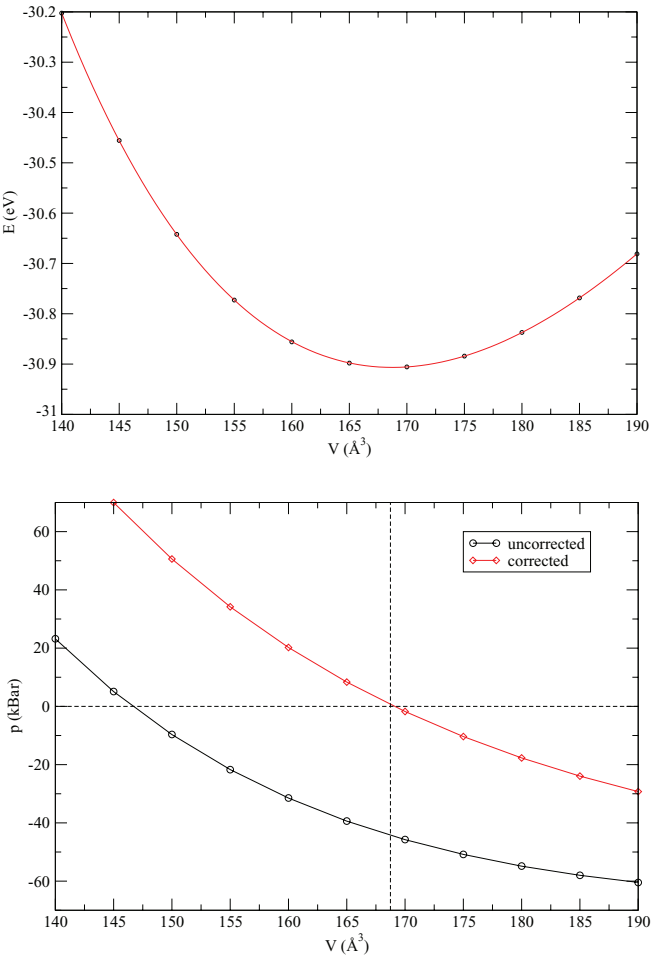

FIG. 1. (Color online) Energy versus volume (above) and internal pressure versus volume (below) curves computed for NaCl using the TS + SCS method with and without gradient corrections. The vertical dashed line marks the minimum in the total energy which must coincide with the volume for which the internal pressure vanishes.

As can be seen, if the uncorrected stress tensor is used in the structural optimization; the predicted volume, i.e., the value for which the uncorrected $p^{\rm int}$ is zero, is $V_0 = 147\ \text{Å}^3$. The error due to the neglect of the structure dependence of the polarizability matrix in the evaluation of the stresses is as large as 20 Å^3 for the equilibrium volume. In calculations with the correct stress tensor, the volume for which the internal pressure $p^{\rm int}$ vanishes coincides with V_0, the position of the energy minimum. Hence the dependence of the polarizability matrix on atomic positions must be taken into account to achieve reliable structural predictions using the TS + SCS method. Based on earlier work of Ángyán *et al.*[46] we derived analytical formulas for energy gradients and stress tensor, which we report together with details of their derivation in the Supplemental Material.[47]

All calculations presented in this work have been performed using the VASP code[34–38] performing a variational solution of the Kohn-Sham equations of DFT in a plane-wave basis. The exchange-correlation energy was determined using the Perdew-Burke-Ernzerhof (PBE) functional.[42] Atomic coordinates and the shape of the unit cell at fixed volume have

TABLE I. Summary of simulation parameters used in this study.

System	k-point mesh	Plane-wave cutoff (eV)
Rare gas solids	$8 \times 8 \times 8$	1000
α-N_2	$8 \times 8 \times 8$	1000
α-N_2	$8 \times 8 \times 8$	1000
SO_2	$5 \times 5 \times 5$	600
Benzene	$2 \times 2 \times 2$	800
Naphthalene	$2 \times 2 \times 2$	1000
Cytosine	$1 \times 1 \times 3$	800
Graphite	$16 \times 16 \times 8$	1000
h-BN	$16 \times 16 \times 8$	1500
V_2O_5	$4 \times 8 \times 8$	1500
MoS_2, $NbSe_2$	$8 \times 8 \times 8$	1500
Se, Te	$6 \times 6 \times 6$	800
Cellulose I-β	$2 \times 1 \times 1$	800
NaCl, KI	$16 \times 16 \times 16$	500
Ni	$19 \times 19 \times 19$	600
Zn, Cd	$25 \times 25 \times 14$	1500

been optimized simultaneously using an automated relaxation procedure, while equilibrium volumes and bulk moduli have been found by fitting the energies at different volumes to a Murnaghan equation of state.[48] Important simulation details such as the number of k-points and the plane-wave cutoff that have been used in our calculations are summarized in Table I. As a test of our implementation of the TS and TS + SCS methods, calculations of isotropic C_6 coefficients for a set of 1225 atomic and molecular dimers (for details see Ref. 22) have been performed. The computed values for the mean absolute relative error with respect to the reference data are 5.3% for TS and 6.2% for TS + SCS. These results are very close to the values of 5.5% and 6.3% reported by Tkatchenko *et al.*[32] with TS and TS + SCS, respectively.

III. RESULTS AND DISCUSSIONS

A. Noble-gas solids

Noble-gas solids are prototypical van der Waals compounds, therefore they are the most obvious candidates for testing and benchmarking any correction scheme for dispersion forces. These systems represent an interesting test of the TS method because the charge distribution of an atom in a noble-gas crystal is almost identical to that of the noninteracting free atom and the volume ratio $\frac{V_A^{\text{eff}}}{V_A^{\text{free}}}$ is therefore close to unity. Consequently, the C_6 coefficients, polarizabilities, and van der Waals radii used in the TS method are basically identical to the free-atomic values.

Our computational results are summarized in Table II and compared with some previous calculations and the available experimental data. In the case of neon, our computed equilibrium lattice parameter is found to be in reasonable agreement with experiment (4.44 Å versus 4.46 Å) and the corresponding cohesive energy of 42 meV/atom is better than the PBE-D2 result (58 meV/atom). Nevertheless, this value is still too large in comparison with experiment (20 meV/atom). Obviously, this is a consequence of the fact that already DFT calculations with the PBE functional predict an attractive interaction between the Ne atoms, with a cohesive energy similar to

TABLE II. Computed equilibrium lattice constants, bulk moduli, and cohesive energies for face-centered cubic noble-gas crystals compared with results from previous theoretical studies and with available experimental data.

Element	Method	a (Å)	B_0 (GPa)	ΔE_{coh} (meV/atom)	Refs.
Ne	Expt.	4.464	1.17	20	96,97
	RPA	4.5	n.a.	17	2
	PBE	4.56	1	20	63
	D2	4.23	4	58	63
	TS	4.42	2.9	43	28
	TS	4.44	2.8	42	
	TS + SCS	4.49	2.6	40	
Ar	Expt.	5.300	2.7	80	98,99
	RPA	5.3	n.a.	83	2
	PBE	5.92	<1	22	63
	D2	5.38	3	88	63
	TS	5.51	2.7	83	28
	TS	5.52	3.1	85	
	TS + SCS	5.60	2.8	80	
Kr	Expt.	5.646	3.6	116	99–101
	RPA	5.7	n.a.	112	2
	PBE	6.49	<1	25	63
	D2	5.64	4	145	63
	TS	5.90	2.6	97	28
	TS	5.92	3.1	106	
	TS + SCS	6.01	2.9	99	
Xe	Expt.	6.132	3.6	164	99,102,103
	PBE	7.01	<1	28	63
	D2	6.06	6	218	63
	TS	6.37	2.4	117	28
	TS	6.38	3.2	140	
	TS + SCS	6.48	3.0	132	

the experimental value. Hence the extra contribution from TS dispersion correction necessarily leads to an overestimation of the computed cohesive energy. For the other three noble-gas elements, the TS method overestimates equilibrium lattice parameters, but the bulk moduli and cohesive energies are reproduced reasonably well (see Table II). A more detailed analysis of the performance of TS method for noble-gas solids, including a discussion of the role of the zero-point energy, has been presented recently by Al-Saidi *et al.*.[28] We note that the small differences in the numerical results reported here and those of Al-Saidi *et al.*[28] (see Table II) are most likely due to the use of slightly different reference data for the free atoms.

As expected, the screening effect included in the TS + SCS method is small for the noble-gas solids. The values of the C_6 coefficients are almost identical to those determined with the TS approach. The only reason why the TS + SCS results (reported in Table II) differ from the TS values is the different value of the scaling parameter s_R (see Sec. II), fit to the interaction energies computed for the S22 reference set[45] using high-level quantum-chemical techniques.

Although the approximate dispersion-correction schemes discussed in this study provide a better description of the structure and energetics of noble-gas solids than standard PBE calculations, these methods do not reach an accuracy comparable to that of the random phase approximation (RPA),

TABLE III. Computed and experimental lattice parameter (a), length of bond between nitrogen atoms in the N_2 molecule (r_{N-N}), bulk modulus (B_0), and cohesive energy (ΔE_{coh}) for α-N_2.

Method	a (Å)	r_{N-N} (Å)	B_0 (GPa)	ΔE_{coh} (kJ/mol)	Refs.
Expt.	5.649	1.066	n.a.	7.6	49,50
PBE	6.19	1.112	<1	2.6	63
D2	5.65	1.112	2.4	8.5	63
TS	5.65	1.112	3.0	9.4	28
TS	5.66	1.112	3.3	9.5	
TS + SCS	5.72	1.112	2.8	8.4	

which reproduces both equilibrium lattice parameters and binding energies[2] very well, but obviously at a much higher computational effort.

B. Molecular solids

Molecular solids represent a class of materials whose calculated cohesive and structural properties depend very critically on a correct description of dispersion interactions. The structural details of these systems are determined by a delicate balance between repulsive and dispersive interactions, as well as electrostatic and induction forces. One should keep in mind that even in case of apolar molecular subunits (like N_2 or benzene) electrostatic forces (in these examples quadrupole-quadrupole interactions) compete with dispersion forces. Therefore the accurate description of the charge distribution by the underlying DFT method (in our case PBE) is an important aspect in an analysis of the results.

In this section, calculations are described for α-N_2 as an example of crystal built by nonpolar molecules and crystalline SO_2 as a prototype of a molecular crystal consisting of polar molecules. In addition, we performed calculations for crystalline benzene and naphthalene, i.e., for crystals built by molecules with no permanent dipole but significant quadrupole moments. Finally, the performance of the TS and TS + SCS methods is examined on crystalline cytosine as an example of a crystal formed by complex organic molecules. We note that DFT calculations with the PBE functional fail badly in the description of all these structures. The computational results are compiled in Tables III to VII; for the sake of brevity, the PBE results will not be discussed in the text.

1. α-N_2

The α phase of N_2 crystallizes in a simple cubic structure with a lattice parameter of 5.694 Å.[49] The N_2 molecules are held together by rather weak interactions; the measured heat of sublimation (7.6 kJ/mol[50]) can serve as an estimate of the cohesive energy. In Table III the results obtained using different methods are compared with experimental data. The TS method performs rather well: the computed lattice parameter a differs by less than 1% from the experimental value and the cohesive energy is only 1.8 kJ/mol larger than the experimentally measured heat of sublimation. The length of the N–N bond is determined by the exchange-correlation functional used in the DFT calculations and is independent of the dispersion corrections. In our best knowledge, the experimental bulk modulus is not available but the value computed using the TS method ($B_0 = 3.3$ GPa) is larger than the PBE-D2 value ($B_0 = 2.4$ GPa). The screening effects play only a minor role for crystalline α-N_2. The lattice parameter computed using TS + SCS is larger only by 0.03 Å, the cohesive energy is lower by 1 kJ/mol, and the bulk modulus is reduced by 0.5 GPa compared to the TS method.

2. Sulfur dioxide

Crystalline sulfur dioxide is an example of a simple crystal built of polar molecules, with a dipole moment of 1.63 D per isolated SO_2 molecule.[51] Sulfur dioxide crystallizes in space group Aba, the unit cell is orthorhombic and contains four SO_2 molecules ($Z = 4$).[52] Experimental and theoretical data are collected in Table IV. Our results show that the dispersion-correction schemes significantly improve the predictions of lattice geometries and cohesive energies compared to the DFT results. The intramolecular parameters (S–O bond length and O–S–O bond angle), on the other hand, are controlled mainly by the exchange-correlation functional and change only slightly if different dispersion corrections are added. Direct comparison of the TS and D2 correction schemes shows that the semi-empirical D2 method performs better in this case: the deviation of the lattice parameters from experiment is only about half the error with the TS method. The TS + SCS results differ from the TS values only moderately: the lattice parameters b and c computed using TS + SCS are larger by 0.01 Å and 0.03 Å, respectively, while a is smaller than the value obtained with the TS method by 0.03 Å. The bulk modulus and the cohesive energy are almost unaffected by screening effects.

3. Benzene and naphthalene

The most stable low-temperature–low-pressure phase I of benzene is orthorhombic and belongs to the space group $Pbca$. The molecules are held together mainly by electrostatic quadrupole-quadrupole interactions and dispersive forces.

TABLE IV. Experimental and theoretical equilibrium volume, lattice constants, intramolecular S–O distance, bulk modulus, and cohesive energy for crystalline sulfur dioxide.

Method	V (Å^3)	a (Å)	b (Å)	c (Å)	r_{S-O} (Å)	α_{O-S-O} (deg.)	B_0 (GPa)	ΔE_{coh} (kJ/mol)	Refs.
Expt.	221.4	6.07	5.94	6.14	1.45	119	n.a.	29	52,104
PBE	268.9	6.41	6.20	6.77	1.451	117.6	2.8	17	
D2	228.3	6.12	5.99	6.23	1.452	117.0	7.5	33	
TS	238.0	6.21	6.02	6.36	1.451	117.1	5.8	35	
TS + SCS	238.4	6.18	6.03	6.39	1.451	118.6	6.0	35	

TABLE V. Calculated and experimental equilibrium volume, lattice parameters, bulk modulus, and cohesive energy for crystalline benzene.

Method	V (Å^3)	a (Å)	b (Å)	c (Å)	B_0 (GPa)	ΔE_{coh} (kJ/mol)	Refs.
Expt.	465.6	7.355	9.371	6.699	8	43–47	53,54,105
EXX/RPA					7.5	47	55
PBE	615.3	8.05	10.15	7.53	1	9.7	63
D2	420.3	7.09	9.07	6.54	10	55.7	63
TS	461.7	7.38	9.20	6.80	10	65.1	28
TS	456.6	7.29	9.15	6.84	10	66.4	
TS + SCS	464.0	7.33	9.26	6.83	10	61.4	

Computational results for benzene are presented in Table V. For the lattice parameters the TS method provides clearly better results than D2. Even for the most problematic parameter b the discrepancy from experiment if strongly reduced from 0.3 Å (D2) to 0.17 Å (TS). However, while TS strongly overestimates the cohesive energy of benzene (the computed value is 18 kJ/mol higher than the heat of sublimation of 47 kJ/mol measured experimentally[53]), D2 leads to a smaller error of about 9 kJ/mol. The bulk moduli of 10 GPa computed using both the D2 and TS methods are reasonably close to the measured value of 8 GPa.[54] Taking into account the screening effects (TS + SCS) leads to an improved lattice geometry. In particular, the lattice parameter b increases by 0.11 Å reducing the error with respect to the experiment to ∼0.1 Å. The value of cohesive energy is also improved, ΔE_{coh} decreases to ∼61 kJ/mol, which is still ∼14 kJ/mol too large compared to the experimental estimate. Tkatchenko *et al.* have shown[32] that the cohesive energy is reduced further if many-body (MB) effects are taken into account. The method that includes both the SCS and MB effects predicts $\Delta E_{coh} = 55$ kJ/mol, similar to the PBE-D2 value. However, the calculation has been performed for the frozen experimental benzene geometry and it is not clear if this result would remain valid if a structural optimization were performed. We note that the treatment of many-body effects is a general problem of the correction schemes considered in this work. Although the energy expressions are based on pairwise interactions in both cases, some many-body effects are included in the self-consistent screening (SCS) procedure. The high-level RPA calculations of Lu *et al.*[55] predict a cohesive energy of 47 kJ/mol and a bulk modulus of 8 kJ/mol, both in excellent agreement with experiment.

Naphthalene crystallizes in a monoclinic structure;[56] the experimentally measured lattice parameters are $a = 8.03$ Å, $b = 5.89$ Å, $c = 8.57$ Å, and $\beta = 123.6°$.

The computed and experimental data are collected in Table VI. As already pointed out by Al-Saidi *et al.*,[28] the TS method improves greatly over the D2 method as far as the structure is concerned, but the predicted cohesive energy is significantly overestimated: ∼100 kJ/mol (TS) versus a measured sublimation heat of 70.4 kJ/mol.[57] As for benzene, TS + SCS leads to a slight reduction of the cohesive energy, but the computed $E_{coh} = 93$ kJ/mol is still too large compared to experiment. All correction schemes considered in this study have a tendency to overestimate the bulk modulus of the naphthalene crystal and the screening seems to have only a very small effect on the computed value of this property.

4. Cytosine

Cytosine is one of the four DNA bases and crystallizes in the space group $P2_12_12_1$ (orthorhombic) with the following cell parameters:[58] $a = 13.041$ Å, $b = 9.494$ Å, $c = 3.815$ Å. The cohesive energy can be estimated from a measured heat of sublimation of 155.0 kJ/mol.[59] As for all other molecular crystals studied in this work, the inclusion of any of the dispersion-correction schemes leads to much more accurate structural and cohesive properties than simple DFT calculations. As obvious from the computed data presented in Table VII, the TS scheme predicts very reasonable values for the lattice parameters, but overestimates the cohesive energy. Inclusion of screening further improves the lattice geometry and decreases the cohesive energy by ∼5 kJ/mol and the bulk modulus by 4 GPa to values comparable with the D2 results. However, the calculated cohesive energy is still more than 10 kJ/mol larger than the experimental value.

C. Layered materials and chain-like structures

The layered materials examined in this section constitute an excellent test of transferability for the parameters of

TABLE VI. Calculated and experimental equilibrium volume, lattice parameters, bulk modulus, and cohesive energy for crystalline naphthalene.

Method	V (Å^3)	a (Å)	b (Å)	c (Å)	β (deg.)	B_0 (GPa)	ΔE_{coh} (kJ/mol)	Refs.
Expt.	337.6	8.03	5.89	8.57	123.6	6.7	70.4	56,57
PBE	n.a	9.15	6.41	9.04	n.a.	1.3	8.6	28,106
D2	n.a.	7.81	5.85	8.50	n.a.	12	74.8	28
TS	n.a.	8.01	5.90	8.62	n.a.	12	95.5	28
TS	340.8	8.03	5.93	8.64	124.1	12	99.6	
TS + SCS	343.3	8.00	5.99	8.68	124.4	12	93.1	

TABLE VII. Computed and experimental equilibrium volume, lattice parameters, bulk modulus, and cohesive energy for crystalline cytosine.

Method	V (Å^3)	a (Å)	b (Å)	c (Å)	B_0 (GPa)	ΔE_{coh} (kJ/mol)	Refs.
Expt.	472.3	13.041	9.494	3.815	n.a.	155.0	58,59
PBE	606.2	12.00	9.50	5.32	4	105.9	63
D2	445.6	12.93	9.46	3.64	14	162.5	63
TS	456.8	12.98	9.46	3.72	18	171.2	28
TS	458.6	13.02	9.44	3.73	19	172.4	
TS + SCS	469.7	13.02	9.47	3.81	14	167.7	

dispersion-correction schemes. Like for molecular crystals, the dispersion interactions play a crucial role in stabilizing the crystal structure of layered materials. Note however, that these materials are chemically very different from the relatively small molecular complexes included in the S22 test set[45] used to optimize the empirical parameter s_R. As we shall see, in spite of their different chemical nature the parameters derived from the S22 set prove to be reasonably well transferable.

1. *Graphite*

Graphite crystallizes in a hexagonal lattice with lattice parameters $a = 2.46$ Å and $c = 6.71$ Å.[60] Although no direct measurement of the interlayer binding energy (E_{bind}) has been performed so far, some information on E_{bind} is available from desorption experiments of polyaromatic molecules from a graphite surface,[61] leading to an estimated value of the interlayer binding energy of 52 meV/atom. The measured bulk modulus is 34–42 GPa.[60,62]

Graphite represents a prototype system for testing the performance of different computational methods capable of treating dispersion interactions, hence a vast amount of computational data is available in the literature. We have shown in our previous study[63] that the D2 method underestimates the lattice parameter c but yields a reasonable interlayer binding energy (55 meV/atom). The van der Waals density functional vdW-DF2[8] predicts a reasonable E_{bind} but overestimates c. Finally, the high-level RPA method[64] predicts structure, binding energy, and bulk modulus that are in excellent agreement with experiment.

In Table VIII, the computational results are compared with experimental data. Evidently, the parameter a determining the distance between carbon atoms within the same layer depends only on the choice of the exchange-correlation functional and is almost unaffected by the dispersion corrections. The TS method yields very reasonable estimate of the lattice parameter c, but the interlayer binding energy is overestimated almost by a factor of two ($E_{\text{bind}} = 82$ meV/atom). A similar result has recently been reported by Hanke[65] ($E_{\text{bind}} = 85$ meV/atom). The computed bulk modulus is by ∼13 GPa too large compared to experiment.[62] The role of screening effect on the cohesion of graphene layers in graphite is massive: as shown in Fig. 2, the C_6 dispersion coefficient changes significantly with the interlayer distance if screening is taken into account, from ∼25 a.u. for $d = 3.35$ Å (the value found in stable graphite) to ∼120 a.u. for $d = 30$ Å. The TS method, on the other hand, predicts only a very small variation of C_6 with d. The difference between C_{6CC}^{TS} and $C_{6CC}^{\text{TS+SCS}}$ increases with increasing interlayer separation. TS + SCS predicts an interlayer binding energy reduced by ∼27 meV/atom compared to TS. The resulting value of $E_{\text{bind}} = 55$ meV/atom is in reasonable

TABLE VIII. Computed and experimental equilibrium lattice parameters, bulk moduli, and interlayer binding energy for graphite and hexagonal boron nitride.

Compound	Method	a (Å)	c (Å)	B_0 (GPa)	ΔE_{bind} (meV/atom)	Refs.
Graphite	Expt.	2.462	6.707	34–42	44	60–62,107
	RPA		6.68	36	48	64
	PBE	2.47	8.84	1	1	63
	D2	2.46	6.45	38	55	63
	vdW-DF2		6.96		53	108
	TS	2.46	6.65	56	n.a.	28
	TS	2.46	6.68	59	82	
	TS + SCS	2.46	6.75	43	55	
h-BN	Expt.	2.503	6.661	37	n.a.	68,69
	RPA	n.a.	6.60	n.a.	39	1,67
	PBE	No binding	No binding	No binding	No binding	63
	D2	2.51	6.17	56	77	63
	TS	n.a.	6.66		86	24
	TS	2.51	6.71	37	n.a.	28
	TS	2.50	6.64	36	87	
	TS + SCS	2.50	6.67	34	73	

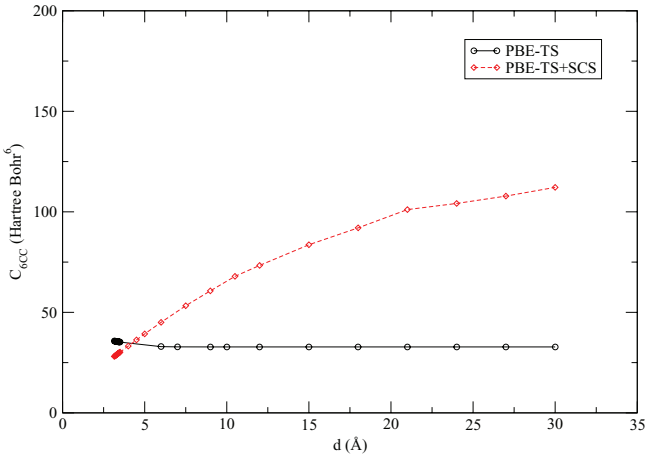

FIG. 2. (Color online) Dispersion coefficient of carbon in graphite computed using PBE-TS and PBE-TS + SCS as a function of interlayer separation d.

agreement with experiment and almost identical to the D2 value. A similar tendency has been reported very recently in the work of Dappe *et al.*,[66] who used a local-orbital DFT combined with second-order many-body perturbation theory and found that additional inclusion of dynamical screening effects reduced the dispersion interaction between graphene layers by 27 meV/atom. In spite of this improvement, the cohesion energy reported in Ref. 66 remained still too large. The bulk modulus of 43 GPa computed using TS + SCS compares well with the available experimental value. Altogether, long-range screening effects have only a modest influence on the lattice geometry of graphite, but they are very important to achieve an interlayer binding energy and bulk modulus in agreement with experiment.

2. *Hexagonal boron nitride*

Hexagonal boron nitride (h-BN) is a layered material structurally similar to graphite, but its physical properties are markedly different: while graphite is a semimetal, h-BN is a large-band-gap insulator. The two materials differ also in the stacking sequence of the hexagonal layer: graphite adopts an AB stacking sequence with the atoms of the B layer located above the center of the hexagonal rings of the A layer, while for h-BN the layers are stacked exactly on top of each other, with each boron atom binding to two nitrogen atoms in the two neighboring layers, and vice versa (AA′ stacking). The small number of atoms per cell has enabled calculations in the random phase approximation (RPA): the calculated[1] out-of-plane lattice parameter was found to be 6.60 Å; within 1% of the experimental value. The corresponding theoretical interlayer binding energy (39 meV/atom) was published only recently.[67]

Our computational results are presented in Table VIII together with some previous theoretical data and the available experimental values. As we noticed earlier[63] the DFT calculations with the PBE functional do not even predict binding between the layers. The D2 method gives a too small interlayer distance (or c lattice parameter) and the binding energy (77 meV/atom) is overestimated with respect to the RPA value. The equilibrium geometries obtained with the TS or the TS + SCS methods are in very good agreement with experiment: $a = 2.50$ Å (TS and TS + SCS), $c = 6.64$ Å (TS), 6.67 Å (TS + SCS), compared with experiment:[68] $a = 2.503$ Å and $c = 6.661$ Å. The calculated bulk moduli (36 GPa with TS and 34 GPa with TS + SCS) are also in good agreement with the experimental value of 37 GPa (Ref. 69). In comparison to the RPA, both TS and TS + SCS strongly overestimate the interlayer binding energy. Our computed TS values are in good agreement with the results reported previously[24,28] using the same computational approach. The slight differences are probably related to different computational setups and some finer details of the implementation.

3. *Vanadium pentoxide*

Another layered material considered in our study is vanadium pentoxide, V_2O_5, crystallizing in an orthorhombic lattice with $a = 11.51$ Å, $b = 3.56$ Å, and $c = 4.37$ Å.[70] The experimental and computational results for V_2O_5 are compiled in Table IX. In our previous PBE + D2 study[63] we found the a and c lattice parameters to be slightly overestimated (see Table IX), while the b parameter was found to be too short compared to experiment. The TS method predicts very reasonable values for the parameters b and c (with errors of less than ∼0.02 Å), while the value of a is still overestimated by 0.16 Å. The self-consistent screening reduces the error for a to 0.08 Å, while the error in the lattice parameter c is increased to 0.14 Å. The inclusion of long-range screening also leads to a reduction of the bulk modulus from 38 to 30 GPa, which is much lower than the experimental value of 50 GPa.[71] We note that the D2 method also predicts a much too low bulk modulus (33 GPa).[63] The V-O distances within the V_2O_5 layers are almost independent of the dispersion corrections (see Table X), which lead to a strong reduction of the interlayer spacing d. Screening leads to an enhanced value of d (comparable to the D2 result) in worse agreement with experiment compared to the TS method.

TABLE IX. Calculated and experimental equilibrium volume, lattice parameters, and bulk modulus for V_2O_5.

Method	V (Å^3)	a (Å)	b (Å)	b/a	c (Å)	c/a	B_0 (GPa)	Refs.
Expt.	179.2	11.512	3.564	0.310	4.368	0.379	50	70,71
PBE	199.0	11.54	3.57	0.310	4.83	0.419	10	
D2	183.7	11.64	3.53	0.303	4.47	0.384	33	63
TS	n.a.	11.68	n.a.	n.a.	4.35	0.372	38	28
TS	179.8	11.67	3.54	0.304	4.35	0.373	38	
TS + SCS	186.2	11.59	3.56	0.307	4.51	0.389	30	

TABLE X. Interatomic distances between vanadium and oxygen atoms and interlayer separation d in vanadium pentoxide. The experimental values are from Ref. 70.

	Expt.	PBE	D2	TS	TS + SCS
V-O(1) (Å)	1.58	1.61	1.61	1.61	1.61
V-O(2) (Å)	1.78	1.78	1.79	1.78	1.79
V-O(3) (Å)	1.88, 2.02	1.88, 2.06	1.89, 2.04	1.87, 2.05	1.88,2.04
d (Å)	2.79	3.23	2.86	2.74	2.89

4. MoS_2 and $NbSe_2$

Molybdenum disulfide (MoS_2) and niobium diselenide ($NbSe_2$) crystallize in layered structures with hexagonal symmetry. The layers are bound to each other by dispersive forces in such a way that cations (Mo or Nb) of a given layer are above the anions (S or Se) of the nearest layers, and vice versa. The band structure and density of states of isolated layers of MoS_2 and $NbSe_2$ were presented recently,[72] while their binding was studied with several methods[6,63,67] taking into account van der Waals interactions. As experimental reference for MoS_2 we use measurements of Bronsema *et al.*[73] (lattice parameters), Aksoy *et al.*[74] (bulk modulus); while the cohesive energy has been reported from the Handbook of Chemistry and Physics (76th ed.) by Raybaud *et al.*.[75] For $NbSe_2$, only experimental structural data are available,[76] while experimental values for the bulk modulus and the cohesive energy have not been reported. Our results are presented in Table XI. As noticed earlier,[63,67,77] the PBE functional strongly overestimates the distance between the layers. The PBE-D2 method cures part of the problem,[63] albeit giving still too large out-of-plane lattice parameters for both MoS_2 and $NbSe_2$. The opposite is true with the TS and TS + SCS methods: the equilibrium cell parameters are found to be smaller than the experimental values: for MoS_2, the computed values of c are 12.03 Å using the TS method and 12.01 Å with the TS + SCS method (to compare with the experimental value[73] of 12.294 Å), and for $NbSe_2$, $c = 12.06$ Å with the TS method and $c = 12.15$ Å with the TS + SCS method (in comparison with 12.482 Å from experiment[76]). For MoS_2, the values of bulk modulus obtained with TS (41 GPa) and with the TS + SCS method (43 GPa) are found to be slightly larger than the corresponding PBE-D2 value (39 GPa), leading to a bit better agreement with experiment[74] (53.4 GPa). For $NbSe_2$, the TS and TS + SCS values of bulk modulus (45 GPa and 54 GPa, respectively) are again close to B_0 obtained with PBE-D2, although the difference is larger than that for MoS_2. All dispersion-corrected schemes examined in this study tend to overestimate cohesive energies: the computed values are 5.37 eV/atom (PBE-D2), 5.33 eV/atom (TS), and 5.31 eV/atom (TS + SCS), while the experimental value[75] is 5.18 eV/atom. For $NbSe_2$, both the TS and TS + SCS methods predict a value of 5.29 eV/atom, which is very close to the PBE-D2 value of 5.27 eV/atom. As to our knowledge, the experimental value of cohesive energy for $NbSe_2$ is not available.

D. Materials with chain-like structures

In this section we describe the calculations performed on systems consisting of covalently bonded chains of atoms or molecules where dispersion interactions are important for providing interchain cohesion. The γ phases of selenium and tellurium consist of helical chains of atoms interacting with each other via van der Waals forces. The β phase of cellulose I is a more complex material: here the dispersion interactions are important for the stacking of two-dimensional sheets of hydrogen-bonded D-glucopyranosyl chains. Hence a reasonably accurate description of three types of interactions: covalent bonds, hydrogen bonds, and dispersion interactions, is necessary for the correct prediction of structural and cohesive properties.

1. Selenium and tellurium

The γ phases of selenium and tellurium crystallize in a hexagonal lattice with space group $P3_121$. The helical chains forming the crystal structure are characterized by the internal parameter u related to the radius q of the helix via the relation[78] $u = (q/a)$. In Tables XII and XIII, the properties calculated with the TS and TS + SCS methods are presented and compared with available experimental data[78] and with other calculations.[63] PBE calculations underestimate both lattice parameters and produce a much too low bulk modulus for Se, but lead to quite good agreement with experiment for Te. Dispersion corrections reduce the lattice parameter

TABLE XI. Computed and experimental structural parameters, bulk moduli, and cohesive energies for MoS_2 and $NbSe_2$ (space group $P6_3/mmc$).

Compound	Method	V (Å^3)	a (Å)	c (Å)	c/a	z	B_0 (GPa)	ΔE_{coh} (eV/atom)
MoS_2	Expt[73]	106.3	3.160	12.294	3.891	0.121	53[74]	5.18[75]
	PBE[63]	128.8	3.18	14.68	4.616	0.143	2	5.12
	PBE + D2[63]	109.4	3.19	12.42	3.893	0.125	39	5.37
	TS	103.9	3.16	12.03	3.81	0.120	41	5.33
	TS + SCS	104.0	3.16	12.01	3.79	0.119	43	5.31
$NbSe_2$	Expt[76]	127.9	3.440	12.482	3.628	0.116		
	PBE[63]	145.0	3.49	13.78	3.948	0.128	6	4.95
	PBE + D2[63]	132.6	3.46	12.76	3.688	0.118	42	5.27
	TS	124.4	3.45	12.06	3.496	0.111	45	5.29
	TS + SCS	125.4	3.45	12.15	3.518	0.111	54	5.29

TABLE XII. Experimental and computed equilibrium volume, lattice constants, internal parameter u, and bulk modulus for selenium and tellurium in the γ phase.

Element	Method	V (Å^3)	a (Å)	c (Å)	c/a	u	B_0 (GPa)	Refs.
Se	Expt.	81.9	4.368	4.958	1.135	0.225	15	78
	PBE	89.3	4.52	5.04	1.115	0.219	4	63
	D2	80.5	4.27	5.10	1.194	0.232	8	63
	TS	78.8	4.22	5.11	1.212	0.237	16	
	TS + SCS	79.6	4.24	5.11	1.206	0.235	14	
Te	Expt.	101.7	4.451	5.926	1.331	0.263	19	78
	PBE	104.8	4.50	5.96	1.324	0.270	18	63
	D2	98.1	4.33	6.04	1.395	0.277	23	63
	TS	100.2	4.42	5.93	1.341	0.278	28	
	TS + SCS	100.7	4.42	5.95	1.345	0.277	26	

a and increase c, improving the agreement of the calculated atomic volume for both elements. The c/a ratio is strongly increased by the dispersion corrections for Se, but less for Te. A relevant structural parameter is the ratio between the interchain and intrachain distances between the atoms, d_2/d_1 (see Table XIII). DFT calculations yield a lower d_2/d_1 ratio than experiment, indicating that the strength of the dispersion forces is overestimated. The difference is very significant for Se, and smaller for Te. Dispersion corrections lead to a further slight reduction of d_2/d_1. The TS method does not perform significantly better than the D2 method: it predicts better structural parameters for Te and a more accurate bulk modulus for Se, but D2 does better for the crystal structure of Se and the bulk modulus of Te. Long-range screening affects the structural parameters only moderately, the difference with respect to the experimental data is only slightly lower than with the TS method. The effect of screening is most obvious for the bulk modulus that is reduced by ∼2 GPa compared to PBE-TS improving slightly the agreement with experiment, which is very good for Se but rather modest for Te.

2. *Cellulose I-β*

Cellulose I-β crystallizes in the space group P112$_1$; the crystallographic unit cell is monoclinic ($a = 7.64$ Å, $b = 8.18$ Å, $c = 10.37$ Å, $\gamma = 96.5°$), and it contains two disaccharide units ($Z = 2$). Sheets formed by H-bonded D-glucopyranosyl chains are stacked perpendicular to the bc plane, the lattice vector a is therefore the most sensitive to the description of dispersion interactions. Reliable descriptions of interactions between D-glucopyranosyl chains in cellulose are important not only for correct structural predictions but are also prerequisite for understanding the thermal behavior and for identification of possible transition mechanisms between different phases of this complex material.[79] In Table XIV, available experimental and theoretical lattice parameters and bulk moduli are compared. In comparison to uncorrected DFT, which, due to the neglect of dispersion forces, leads to a strong overestimation of the lattice parameter a and of the volume, the D2 and TS methods lead to significantly improved structural properties: both methods predict very similar lengths of lattice vectors, while the TS method gives a slightly better value of lattice angle γ (96.4°) than the D2 method (96.8°). Inclusion of long-range screening in this case leads to a somewhat worse agreement with experimental data than with the TS method. The most significant difference is the increase of lattice angle γ to 97.5°, which is 1° larger that the corresponding experimental value. All three dispersion-correction methods considered in this study predict similar values for bulk modulus: 16 GPa (D2), 19 GPa (TS), and 18 GPa (TS + SCS). The experimental value for B_0 is not available.

TABLE XIII. Experimental and calculated values of intrachain (d_1) and interchain distances (d_2) and bond angle (θ) for selenium and tellurium.

Element	Method	d_1 (Å)	d_2 (Å)	d_2/d_1	θ (deg.)	Refs.
Se	Expt.	2.37	3.44	1.45	103.2	78
	PBE	2.40	3.57	1.386	103.5	63
	D2	2.42	3.37	1.392	104.0	63
	TS	2.43	3.32	1.366	103.8	
	TS + SCS	2.43	3.33	1.370	103.8	
Te	Expt.	2.83	3.49	1.23	103.3	78
	PBE	2.89	3.50	1.211	101.9	63
	D2	2.89	3.40	1.176	103.2	63
	TS	2.90	3.42	1.179	101.2	
	TS + SCS	2.90	3.42	1.179	101.3	

E. Ionic crystals

Although van der Waals forces are usually not considered as important for the cohesive and structural properties of ionic crystals, the results of a recent theoretical study of Zhang *et al.*[80] indicate the opposite: inclusion of dispersion interactions in DFT calculations has been shown to lead to an overall improvement of the cohesive properties of ionic (NaCl, MgO) and semiconducting (Si, Ge, GaAs) solids. Long-range screening has been identified as an important factor affecting the polarizability of atoms in solids.[80] As discussed in the work of Ehrlich *et al.*,[81] the dispersion coefficients of atoms in solids depend strongly on the degree of covalency and on the oxidation state.

In this section we discuss sodium chloride (NaCl) and potassium iodide (KI) as examples for ionic materials. Both

TABLE XIV. Experimental and computed equilibrium volumes, lattice parameters, and bulk modulus of crystalline cellulose I-β.

Method	V (Å^3)	a (Å)	b (Å)	c (Å)	γ (deg.)	B_0 (GPa)	Refs.
Expt.	658.3	7.64	8.18	10.37	96.5	n.a.	109
PBE	744.9	8.70	8.23	10.46	95.5	6	63
D2	642.5	7.65	8.14	10.39	96.8	16	63
TS	642.8	7.63	8.14	10.41	96.4	19	
TS + SCS	646.3	7.68	8.15	10.42	97.5	18	

compounds crystallize in a simple cubic structure in which the lattice sites are occupied alternatingly by cations (alkali metals) and anions (halogen) along the three lattice directions. The computed results are compared with experiment in Table XV. DFT calculations lead to reasonably accurate values for lattice constant, bulk modulus, and cohesive energy for both ionic crystals, albeit the lattice constant for KI is somewhat too large. Interestingly, including dispersion interactions using the D2 method improves the lattice constant and cohesive energy: the error for a is reduced from 0.07 Å (NaCl) and 0.12 Å (KI) obtained using DFT to only 0.03 Å (NaCl) and −0.02 Å (KI) and the error for computed cohesive energies decreases from the DFT values of −0.14 eV/atom (NaCl and KI) to 0.05 eV/atom (NaCl) and 0.12 eV/atom (KI). On the other hand, D2 overestimates bulk modulus by 8 GPa for NaCl and by 4 GPa for KI. The TS method strongly overestimates the strength of dispersion forces, leading to too high cohesive energies (the error with respect to experimental data being 0.66 eV/atom for NaCl and 0.67 eV/atom for KI) and bulk moduli (84 GPa for NaCl, 22 GPa for KI) and strongly underestimates the lattice parameters ($a = 5.34$ Å for NaCl and 6.29 Å for KI). Self-consistent screening has a dramatic influence for ionic crystals: the overestimation of cohesive energy and bulk modulus is significantly reduced and the lattice constants are increased (see Table XV). This result is consistent with the finding of Zhang *et al.*[80] who showed in their theoretical study that long-range electrostatic screening strongly affects the polarizability of atoms in solids. The absolute value of the errors for TS + SCS is comparable with that for DFT, but in the opposite direction. In conclusion, for alkali-metal halides the semi-empirical D2 method leads to better agreement with experiment than the TS or the TS + SCS methods.

TABLE XV. Experimentally measured and computed lattice parameters, bulk moduli, and cohesive energies for NaCl and KI.

Compound	Method	a (Å)	B_0 (GPa)	E_{coh} (eV/atom)	Refs.
NaCl	Expt.	5.63	24	3.31	91,110,111
	PBE	5.70	24	3.17	63
	D2	5.66	32	3.36	63
	TS	5.34	84	3.97	
	TS + SCS	5.53	33	3.58	
KI	Expt.	7.07	12	2.72	91,112,113
	PBE	7.19	11	2.58	
	D2	7.05	16	2.84	
	TS	6.29	22	3.39	
	TS + SCS	7.06	14	2.97	

F. Metals

As has been shown earlier in model calculations, the high mobility of electrons in metals leads to strong screening effects, strongly reducing the interaction of fluctuating dipoles. Nevertheless, several examples of non-negligible London dispersion effects in metals have been reported. Tao *et al.*[82] showed that for the heavier alkali metals, dispersion forces may reduce the lattice parameter by as much as 0.1 Å. The role of dispersion forces on the structural and cohesive properties of the divalent post-transition (group 12) metals such as Zn, Cd, and Hg has been discussed by several authors.[83–85] We note that a recent attempt to use dispersion-corrected DFT (PBE-D2) failed to predict correctly the relative stability of the polymorphs of mercury.[86] Strictly speaking, the application of any atoms-in-molecules–based concept to metallic systems is very problematic due to the highly delocalized nature of the electrons. Nevertheless, several computational studies have been already published where the TS method was applied to study the interactions of organic molecules with surfaces of metals.[29,87,88] Although we are aware of the conceptual deficiency, we find it important to examine numerically the performance of different variants of the TS method for this class of materials, too.

1. Nickel

Nickel crystallizes in a face-centered cubic structure with the lattice parameter $a = 3.52$ Å.[89] The measured bulk modulus and cohesive energy are 190 GPa[90] and 4.35 eV/atom,[91] respectively. Experimental and computed properties of Ni are compiled in Table XVI. The values of a and B_0 predicted by DFT calculations with the PBE functional are in very good agreement with experiment, only the cohesive energy is overestimated by 0.52 eV. All dispersion-corrected schemes examined in this study underestimate the value of lattice parameter and overestimate bulk modulus and cohesive energy, the TS method showing the worst performance in this case. Long-range screening improves results significantly compared with the TS method; in particular, the error in a is reduced

TABLE XVI. Experimental and theoretical lattice constants, bulk modulus, and cohesive energy for face-centered cubic nickel.

Method	a (Å)	B_0 (GPa)	E_{coh} (eV/atom)	Refs.
Expt.	3.52	190	4.35	89–91
PBE	3.52	191	4.87	
D2	3.46	214	5.35	
TS	3.44	267	5.77	
TS + SCS	3.49	209	5.40	

TABLE XVII. Experimental and computed equilibrium volume, lattice constants, axial ratio, bulk modulus, and cohesive energy for zinc and cadmium. CCI stands for coupled cluster calculations with the method of increments.

Element	Method	V (Å^3)	a (Å)	c (Å)	c/a	B_0 (GPa)	E_{coh}(eV/atom)	Refs.
Zn	Expt.	29.59	2.654	4.851	1.83	80	1.35	83,84,92
	PBE	31.1	2.65	5.12	1.93	71	1.00	84
	CCI	29.3	2.61	4.98	1.91		1.35	92
	PBE	30.55	2.66	5.00	1.88	54	1.10	
	D2	31.25	2.59	5.37	2.07	60	1.45	
	TS	28.14	2.62	4.75	1.81	78	1.51	
	TS + SCS	29.51	2.63	4.91	1.86	60	1.38	
Cd	Expt.	43.22	2.98	5.62	1.89	62	1.19	84,85
	PBE	45.0	3.02	5.69	1.88	53	0.69	85
	CCI	41.4	2.92	5.61	1.92		1.19	85
	PBE	46.02	3.04	5.76	1.89	37	0.73	
	D2	48.27	3.21	5.42	1.69	39	1.36	
	TS	42.15	2.97	5.51	1.85	50	1.13	
	TS + SCS	45.08	2.96	5.93	2.00	25	1.06	

from 0.08 to 0.03 Å and the error in B_0 is decreased from 76 to 18 GPa. However, the error is still significantly larger than with plain DFT.

2. Zinc and cadmium

The crystal structures of zinc and cadmium have recently excited a lot of interest. Both metals crystallize in a hexagonal closed-packed structure, but the axial ratio c/a differs significantly from the ideal value of 1.63.[83] Moreover, it has been claimed that calculations at the GGA level[84] fail to reproduce accurately the experimental axial ratio values and only methods accounting for electron correlations at the level of coupled cluster theory[85,92] are in reasonable agreement with experiment. The importance of an accurate description of correlation for the properties of metallic Zn and Cd was also discussed in Ref. 93.

Our computed results are presented in Table XVII. As reported before,[84] PBE calculations tend to overestimate the axial ratio of Zn and Cd. However, the discrepancy with respect to experiment for Zn is not as large as reported before, for Cd we even note very good agreement with experiment. The calculated lattice parameters for Zn are $a = 2.66$ Å and $c = 5.00$ Å (experiment: $a = 2.654$ Å, $c = 4.851$ Å). For Cd, the values are $a = 3.04$ Å, $c = 5.76$ Å (PBE), and $a = 2.98$ Å, $c = 5.62$ Å (experiment). PBE predicts too low values for the bulk modulus: 54 GPa (Zn) and 37 GPa (Cd), to be compared with the experimental results of 80 GPa (Zn) and 62 GPa (Cd). The cohesive energies are significantly underestimated: -1.1 eV (PBE) versus -1.35 eV (experiment) for Zn, and -0.73 eV versus -1.19 eV for Cd.

Dispersion corrections based on the semi-empirical D2 method do not clearly improve the results. The computed equilibrium volumes are even larger than predicted by PBE; the cohesive energies are now overestimated. The axial ratio predicted with the D2 correction method is far too large for Zn and far too small for Cd. The TS and TS + SCS methods perform surprisingly well for the crystal structure. For zinc, the TS method predicts an equilibrium volume of 28.14 Å^3, $a = 2.62$ Å, $c = 4.75$ Å and $c/a = 1.81$, for Cd the corresponding values are 42.15 Å^3, $a = 2.97$Å, $c = 5.51$ Å and $c/a = 1.85$, both in reasonable agreement with experiment. The calculated bulk modulus for Zn is 78 GPa, in excellent agreement with experiment (80 GPa), while the cohesive energy is found to be too large compared with experiment (1.51 eV versus 1.35 eV). For Cd the calculated values of both bulk modulus and cohesive energy are lower than experiment (50 GPa versus 62 GPa, and 1.13 eV versus 1.19 eV)

In the case of zinc, the inclusion of the self-consistent screening leads to even better agreement with experimental structural data (equilibrium volume 29.51 Å^3, $a = 2.63$ Å and $c = 4.91$Å, $c/a = 1.86$). The bulk modulus ($B_0 = 60$ GPa) is reduced in comparison with the TS method, but the cohesive energy is improved, with a value very close to experiment ($E_{coh} = -1.38$ eV). For cadmium, screening leads to an increase of the volume and lattice parameter c, leading to a too high value of the axial ratio of $c/a = 2.00$, and a much too low value of the bulk modulus.

These results indicate that the applicability of the TS + SCS method to metals is questionable. We note that an alternative scheme to include screening effects on the C_6 coefficients for metals in the TS method has recently been proposed by Ruiz *et al.*[94] and successfully used to study adsorption of large organic molecules on surfaces of metals.[94,95]

IV. CONCLUSIONS

In this study, the application of the Tkatchenko-Scheffler (TS) method[22] for dispersion corrections to DFT energies and forces to extended systems including noble-gas solids, molecular crystals, layered and chain-like structures, ionic crystals, and metals has been examined. The effect of long-range screening as described by the TS + SCS method[32] has also been investigated. The TS dispersion corrections added to DFT calculations using the gradient-corrected PBE functional method lead to reasonably accurate predictions of the structural and cohesive properties for various kinds of solids, where dispersion forces are expected to be essential. However, a

critical examination shows that the performance is not equally good for all systems and there are some types of solids where the approach definitely fails. For the light noble-gas solids the predicted equilibrium volume is accurate, but the cohesive energy is too large. This changes gradually to an overestimation of the volume and an underestimation of the cohesive energy for the heavier noble gases. For molecular crystals the calculated volume is quite accurate (or slightly too small as for sulfur dioxide and cytosine), the cohesive energy is accurate for nitrogen, but overestimated to some degree for the other systems. For layered crystals the calculated volumes and interlayer distances are quite accurate, but the interlayer binding energy is too large. For chain-like structures the calculated equilibrium volumes and bulk moduli are quite accurate, but for selenium and tellurium the ratio of interchain and intrachain distances between the atoms is underestimated, indicating an overestimation of the strength of the dispersion forces promoting the interchain binding. For strongly ionic systems such as the alkali halide crystals the TS method definitely fails—the calculated lattice constants are far too small, the cohesive energies are too large. For metals the application of a method based on an atom-in-solid concept is obviously questionable. For nickel the addition of TS dispersion corrections destroys the perfect agreement of lattice constant and bulk modulus with experiment achieved at the DFT level and increases the overestimation of the cohesive energy. For the highly anisotropic divalent post-transition metals zinc and cadmium it has been claimed that a description of electronic correlation beyond the DFT level is necessary to achieve an accurate prediction of the axial ratio. For zinc where DFT calculations produce a too large value of c/a and a too low binding energy, the TS method corrects the structure, but the cohesive energy is slightly too large. For cadmium were the DFT result for c/a is quite accurate, the TS correction leads to a too small value of c/a.

The original TS scheme accounts for the influence of the local chemical environment by calibrating the dispersion coefficients according to the atom-in-solid volumes, but it neglects long-range dynamical screening and many-body effects. We have shown that the screening effects are rather small for systems consisting of weakly interacting neutral atoms (noble-gas solids) and molecules. For these systems screening leads to a small expansion of the lattice constants by at most 1%. The cohesive energy is reduced by less than 1% for the noble-gas crystals; for molecular crystals the reduction is almost zero for crystalline SO_2 and varies between -2.7% for cytosine and -13% for α-N_2. The screening effect is most pronounced for layered and chain-like structures. For the layered crystals the interlayer distance is expanded by 0.5% for h-BN, 1% for graphite, and 4% for V_2O_5, the interlayer binding energy is reduced by -50%, -16%, and -20%, respectively. For graphite the screening effect leads to very good agreement of the computed interlayer binding energy of 55 meV/atom with the experimental estimate of 52 meV/atom[61] and the high-level RPA result of 48 meV/atom.[64] For Se and Te screening expands the interchain distances at constant intrachain spacings and reduces the cohesive energy by -12% and -7%, respectively. For ionic crystals the expansion of the lattice constants and the reduction of the cohesive energy goes into the right direction, but the accuracy of TS + SCS calculations does not reach the DFT level. For Zn and Cd the screening effects emphasize the anisotropic character of the structure and lead to reasonably accurate cohesive energies.

Further improvement of the Tkatchenko-Scheffler model can be envisaged in various directions. In our opinion, one should avoid the temptation of introducing further adjustable ingredients, rather one should try to remove the still-persisting arbitrariness in the model. One of the neuralgic points is the calibration of the atomic volumes by the original Hirshfeld partitioning, which is based on the neutral free atomic densities. This is probably a questionable choice for strongly polar or ionic systems: it is difficult to conceive that the polarizability of fully charged ions can be simply scaled from the neutral atomic polarizability. We are currently attempting to remove this arbitrariness by using improved Hirshfeld partitioning methods. Correct treatment of the forces and stresses, taking into account the geometrical derivatives of the many-body dynamical polarizability matrix is absolutely crucial.

ACKNOWLEDGMENTS

The authors are grateful to Dr. Alexandre Tkatchenko for helpful discussions and for providing the atomic reference data. This work has been supported by the VASP project, by project APVV-0059-10, and by ANR (Agence National de Recherche) via contract number ANR-07-BLAN-0272 (Wademecom). T.B. is grateful to the Université de Lorraine, former University of Nancy for the invited professorship during the academic years 2011 and 2012.

APPENDIX: VASP KEYWORDS

The TS and TS + SCS methods are available in the VASP package of version 5.3.3 and later. The TS method in VASP requires the use of new set of POTCAR files, which were released in 2012. The following keywords are used to control this feature:

(1) IVDW = 2 activates the DFT-TS method.

(2) VDW_RADIUS = cutoff radius in Å for the summation in Eq. (1) (default is 30 Å).

(3) VDW_SR = scaling parameter s_R; see Eq. (7) (default is 0.94).

(4) VDW_D = parameter d in the damping function defined in Eq. (7) (default is 20).

(5) The atomic reference data can be optionally defined via flags VDW_alpha (atomic polarizabilities in Bohr^3), VDW_C6 (atomic C_6 coefficients in J nm^6 mol^{-1}), and VDW_R0 (van der Waals radii of noninteracting atoms in Å). When any of these flags are used, the user must provide values for each species present in the system, whereby the order of species must be consistent with that in the POTCAR file.

(6) LVDWSCS if set to .TRUE., C_6, α, and R are corrected for self-consistent screening effect by means of the TS + SCS method.

*tomas.bucko@univie.ac.at
†sebastien.lebegue@crm2.uhp-nancy.fr

[1] A. Marini, P. García-González, and A. Rubio, Phys. Rev. Lett. **96**, 136404 (2006).
[2] J. Harl and G. Kresse, Phys. Rev. B **77**, 045136 (2008).
[3] J. Harl and G. Kresse, Phys. Rev. Lett. **103**, 056401 (2009).
[4] L. Spanu, S. Sorella, and G. Galli, Phys. Rev. Lett. **103**, 196401 (2009).
[5] N. E. Dahlen, R. van Leeuwen, and U. von Barth, Phys. Rev. A **73**, 012511 (2006).
[6] H. Rydberg, M. Dion, N. Jacobson, E. Schröder, P. Hyldgaard, S. I. Simak, D. C. Langreth, and B. I. Lundqvist, Phys. Rev. Lett. **91**, 126402 (2003).
[7] H. Rydberg, B. I. Lundqvist, D. C. Langreth, and M. Dion, Phys. Rev. B **62**, 6997 (2000).
[8] K. Lee, E. D. Murray, L. Kong, B. I. Lundqvist, and D. C. Langreth, Phys. Rev. B **82**, 081101 (2010).
[9] J. F. Dobson and B. P. Dinte, Phys. Rev. Lett. **76**, 1780 (1996).
[10] J. F. Dobson and J. Wang, Phys. Rev. Lett. **82**, 2123 (1999).
[11] J. F. Dobson and J. Wang, Phys. Rev. B **62**, 10038 (2000).
[12] O. A. Vydrov and T. Van Voorhis, Phys. Rev. Lett. **103**, 063004 (2009).
[13] O. A. Vydrov and T. Van Voorhis, J. Chem. Phys. **133**, 244103 (2010).
[14] J. Klimes and A. Michaelides, J. Chem. Phys. **137**, 120901 (2012).
[15] S. Grimme, J. Comput. Chem. **25**, 1463 (2004).
[16] S. Grimme, J. Comput. Chem. **27**, 1787 (2006).
[17] S. Grimme, J. Antony, S. Ehrlich, and H. Krieg, J. Chem. Phys. **132**, 154104 (2010).
[18] A. D. Becke and E. R. Johnson, J. Chem. Phys. **122**, 154104 (2005).
[19] A. D. Becke and E. R. Johnson, J. Chem. Phys. **123**, 154101 (2005).
[20] T. Sato and H. Nakai, J. Chem. Phys. **131**, 224104 (2009).
[21] T. Sato and H. Nakai, J. Chem. Phys. **133**, 194101 (2010).
[22] A. Tkatchenko and M. Scheffler, Phys. Rev. Lett. **102**, 073005 (2009).
[23] F. L. Hirshfeld, Acta Crystallogr., Sect. B: Struct. Crystallogr. Cryst. Chem. **27**, 769 (1971).
[24] N. Marom, A. Tkatchenko, M. Scheffler, and L. Kronik, J. Chem. Theory Comput. **6**, 81 (2010).
[25] N. Marom, J. Bernstein, J. Garel, A. Tkatchenko, E. Joselevich, L. Kronik, and O. Hod, Phys. Rev. Lett. **105**, 046801 (2010).
[26] N. Marom, A. Tkatchenko, S. Kapishnikov, L. Kronik, and L. Leiserowitz, Cryst. Growth Des. **11**, 3332 (2011).
[27] A. Tkatchenko, M. Rossi, V. Blum, J. Ireta, and M. Scheffler, Phys. Rev. Lett. **106**, 118102 (2011).
[28] W. A. Al-Saidi, V. K. Voora, and K. D. Jordan, J. Chem. Theory Comput. **8**, 1503 (2012).
[29] E. R. McNellis, J. Meyer, and K. Reuter, Phys. Rev. B **80**, 205414 (2009).
[30] D. Tunega, T. Bučko, and A. Zaoui, J. Chem. Phys. **137**, 114105 (2012).
[31] F. Göltl, A. Grüneis, T. Bučko, and J. Hafner, J. Chem. Phys. **137**, 114111 (2012).
[32] A. Tkatchenko, R. A. Di Stasio, R. Car, and M. Scheffler, Phys. Rev. Lett. **108**, 236402 (2012).
[33] R. A. DiStasio, Jr., O. A. von Lilienfeld, and A. Tkatchenko, Proc. Natl. Acad. Sci. USA **109**, 14791 (2012).
[34] G. Kresse and J. Hafner, Phys. Rev. B **48**, 13115 (1993).
[35] G. Kresse and J. Hafner, Phys. Rev. B **49**, 14251 (1994).
[36] G. Kresse and J. Furthmüller, Comput. Mater. Sci. **6**, 15 (1996).
[37] G. Kresse and J. Furthmüller, Phys. Rev. B **54**, 11169 (1996).
[38] G. Kresse and D. Joubert, Phys. Rev. B **59**, 1758 (1999).
[39] E. R. Johnson and A. D. Becke, J. Chem. Phys. **124**, 174104 (2006).
[40] F. O. Kannemann and A. D. Becke, J. Chem. Phys. **136**, 034109 (2012).
[41] N. Marom, A. Tkatchenko, M. Rossi, V. V. Gobre, O. Hod, M. Scheffler, and L. Kronik, J. Chem. Theory Comput. **7**, 3944 (2011).
[42] J. P. Perdew, K. Burke, and M. Ernzerhof, Phys. Rev. Lett. **77**, 3865 (1996).
[43] A. Tkatchenko (private communication).
[44] H. B. G. Casimir and D. Polder, Phys. Rev. **73**, 360 (1948).
[45] P. Jurecka, J. Sponer, J. Cerny, and P. Hobza, Phys. Chem. Chem. Phys. **8**, 1985 (2006).
[46] J. G. Ángyán, F. Colonna-Cesari, and O. Tapia, Chem. Phys. Lett. **166**, 180 (1990).
[47] See Supplemental Material at http://link.aps.org/supplemental/10.1103/PhysRevB.87.064110 for analytical formulas for energy gradients and stress tensor used in TS + SCS method and for details of their derivation.
[48] F. Murnaghan, Proc. Natl. Acad. Sci. USA **15**, 244 (1944).
[49] A. F. Schuch and R. L. Mills, J. Chem. Phys. **52**, 6000 (1970).
[50] T. S. Kuan, A. Warshel, and O. Schnepp, J. Chem. Phys. **52**, 3012 (1970).
[51] D. Patel, D. Margolese, and T. R. Dykea, J. Chem. Phys. **70**, 2740 (1979).
[52] B. Post, R. S. Schwartz, and I. Fankuchen, Acta Crystallogr. **5**, 372 (1952).
[53] J. S. Chickos and W. E. Acree, J. Phys. Chem. Ref. Data **31**, 537 (2002).
[54] E. J. Meijer and M. Sprik, J. Chem. Phys. **105**, 8684 (1996).
[55] D. Lu, Y. Li, D. Rocca, and G. Galli, Phys. Rev. Lett. **102**, 206411 (2009).
[56] I. Natkaniec, A. V. Belushkin, W. Dyck, H. Fuess, and C. M. E. Zeyen, Z. Kristallogr. **163**, 285 (1983).
[57] S. N. Vaidya and G. C. Kennedy, J. Chem. Phys. **55**, 987 (1971).
[58] D. L. Barker and R. E. Marsh, Acta Crystallogr. **17**, 1581 (1964).
[59] P. M. Burkinshaw and C. T. Mortimer, J. Chem. Soc., Dalton Trans. **39**, 75 (1984).
[60] Y. X. Zhao and I. L. Spain, Phys. Rev. B **40**, 993 (1989).
[61] R. Zacharia, H. Ulbricht, and T. Hertel, Phys. Rev. B **69**, 155406 (2004).
[62] M. Hanfland, H. Beister, and K. Syassen, Phys. Rev. B **39**, 12598 (1989).
[63] T. Bučko, J. Hafner, S. Lebègue, and J. G. Ángyán, J. Phys. Chem. A **114**, 11814 (2010).
[64] S. Lebègue, J. Harl, T. Gould, J. G. Ángyán, G. Kresse, and J. F. Dobson, Phys. Rev. Lett. **105**, 196401 (2010).
[65] F. Hanke, J. Comput. Chem. **32**, 1424 (2011).
[66] Y. J. Dappe, P. G. Bolcatto, J. Ortega, and F. Flores, J. Phys.: Condens. Matter **24**, 424208 (2012).
[67] T. Björkman, A. Gulans, A. V. Krasheninnikov, and R. M. Nieminen, Phys. Rev. Lett. **108**, 235502 (2012).
[68] R. S. Pease, Acta Crystallogr. **5**, 356 (1952).
[69] V. L. Solozhenko, G. Will, and F. Elf, Solid State Commun. **96**, 1 (1995).
[70] R. Enjalbert and J. Galy, Acta Crystallogr., Sect. C: Cryst. Struct. Commun. **42**, 1467 (1986).

[71]I. Loa, A. Grzechnik, U. Schwarz, K. Syassen, M. Hanfland, and R. K. Kremer, J. Alloys Compd. **317–318**, 103 (2001).
[72]S. Lebègue and O. Eriksson, Phys. Rev. B **79**, 115409 (2009).
[73]K. D. Bronsema, J. L. De Boer, and F. Jellinek, Z. Anorg. Allg. Chem. **541**, 15 (1986).
[74]R. Aksoy, Y. Ma, E. Selvi, M. C. Chyu, A. Ertas, and A. White, J. Phys. Chem. Solids **67**, 1914 (2006).
[75]P. Raybaud, G. Kresse, J. Hafner, and H. Toulhoat, J. Phys.: Condens. Matter. **9**, 11085 (1997).
[76]M. Marezio, P. D. Dernier, A. Menth, and J. G. W. Hull, J. Solid State Chem. **4**, 425 (1972).
[77]M. V. Bollinger, K. W. Jacobsen, and J. K. Nørskov, Phys. Rev. B **67**, 085410 (2003).
[78]R. Keller, W. B. Holzapfel, and H. Schulz, Phys. Rev. B **16**, 4404 (1977).
[79]T. Bučko, D. Tunega, J. G. Ángyán, and J. Hafner, J. Phys. Chem. A **115**, 10097 (2011).
[80]G.-X. Zhang, A. Tkatchenko, J. Paier, H. Appel, and M. Scheffler, Phys. Rev. Lett. **107**, 245501 (2011).
[81]S. Ehrlich, J. Moellmann, W. Reckien, T. Bredow, and S. Grimme, ChemPhysChem **12**, 3414 (2011).
[82]J. Tao, J. P. Perdew, and A. Ruzsinszky, Phys. Rev. B **81**, 233102 (2010).
[83]J. Nuss, U. Wedig, A. Kirfel, and M. Jansen, Z. Anorg. Allg. Chem. **636**, 309 (2010).
[84]U. Wedig, M. Jansen, B. Paulus, K. Rosciszewski, and P. Sony, Phys. Rev. B **75**, 205123 (2007).
[85]N. Gaston, D. Andrae, B. Paulus, U. Wedig, and M. Jansen, Phys. Chem. Chem. Phys. **12**, 681 (2010).
[86]S. Biering and P. Schwerdtfeger, Theor. Chem. Acta **130**, 455 (2011).
[87]G. Mercurio, E. R. McNellis, I. Martin, S. Hagen, F. Leyssner, S. Soubatch, J. Meyer, M. Wolf, P. Tegeder, F. S. Tautz *et al.*, Phys. Rev. Lett. **104**, 036102 (2010).
[88]L. Adamska, R. Addou, M. Batzill, and I. I. Oleynik, Appl. Phys. Lett. **101** (2012).
[89]J. Bandyopadhyay and K. P. Gupta, Cryogenics **17**, 345 (1977).
[90]G. Simmons and H. Wang, *Single Crystal Elastic Constants and Calculated Aggregate Properties: A Handbook* (MIT Press, Cambridge, 1971).
[91]M. W. J. E. Chase, *NIST-JANAF Thermochemical Tables* (AIP Press, New York, 1998).
[92]N. Gaston, B. Paulus, U. Wedig, and M. Jansen, Phys. Rev. Lett. **100**, 226404 (2008).
[93]S. Sculfort and P. Braunstein, Chem. Soc. Rev. **40**, 2741 (2011).
[94]V. G. Ruiz, W. Liu, E. Zojer, M. Scheffler, and A. Tkatchenko, Phys. Rev. Lett. **108**, 146103 (2012).
[95]W. A. Al-Saidi, H. Feng, and K. A. Fichthorn, Nano Lett. **12**, 997 (2012).
[96]D. N. Batchelder, D. L. Losee, and R. O. Simmons, Phys. Rev. **162**, 767 (1967).
[97]G. T. McConville, J. Chem. Phys. **60**, 4093 (1974).
[98]O. G. Peterson, D. N. Batchelder, and R. O. Simmons, Phys. Rev. **150**, 703 (1966).
[99]L. A. Schwalbe, R. K. Crawford, H. H. Chen, and R. A. Aziz, J. Chem. Phys. **66**, 4493 (1977).
[100]D. L. Losee and R. O. Simmons, Phys. Rev. **172**, 944 (1968).
[101]J. Skalyo, Y. Endoh, and G. Shirane, Phys. Rev. B **9**, 1797 (1974).
[102]D. R. Sears and H. P. Klug, J. Chem. Phys. **37**, 3002 (1962).
[103]N. A. Lurie, G. Shirane, and J. Skalyo, Phys. Rev. B **9**, 2661 (1974).
[104]L. Schriver-Mazzuoli, H. Chaabouni, and A. Schriver, J. Mol. Struct. **644**, 151 (2003).
[105]W. I. F. David, R. M. Ibberson, G. A. Jeffrey, and J. R. Ruble, Phys. B (Amsterdam, Neth.) **180**, 597 (1992).
[106]Y. Liu and W. A. Goddard, III, J. Phys. Chem. Lett. **1**, 2550 (2010).
[107]Z. Liu, J. Z. Liu, Y. Cheng, Z. Li, L. Wang, and Q. Zheng, Phys. Rev. B **85**, 205418 (2012).
[108]K. Berland, O. Borck, and P. Hyldgaard, Comput. Phys. Commun. **182**, 1800 (2011).
[109]Y. Nishiyama, G. P. Johnson, A. D. French, V. T. Forsyth, and P. Langan, Biomacromolecules **9**, 3133 (2008).
[110]F. W. C. Boswell, Proc. Phys. Soc., London, Sect. A **64**, 465 (1951).
[111]S. N. Vaidya and G. C. Kennedy, J. Phys. Chem. Solids **32**, 951 (1971).
[112]P. G. Hambling, Acta Crystallogr. **6**, 98 (1953).
[113]G. Barsch and H. Shull, Phys. Status Solidi B **43**, 637 (1971).